Temperature Effect on Transport Performance by Inorganic Nanofiltration Membranes

Toshinori Tsuru, Shuhei Izumi, Tomohisa Yoshioka, and Masashi Asaeda
Dept. of Chemical Engineering, Hiroshima University, Higashi-Hiroshima, 739-8527, Japan

The effect of temperature on nanofiltration performance was examined using three inorganic membranes with a molecular-weight cutoff of approximately 200, 600, and 2,000, respectively. The inorganic porous membranes were prepared from silica-zirconia colloidal sols and used in nanofiltration experiments for neutral solutes over a temperature range of 20 to 60°C. The rejection of solutes decreased with an increase in temperature for the membranes, while the permeate volume flux increased. Three transport coefficients — refection coefficient, solute permeability, and water permeability — were obtained using the Spiegler-Kedem equation, which accounts for the contribution of convection and diffusion to solute flux. As a result, the reflection coefficient corresponding to the fraction of solutes reflected by the membrane in convective flow was almost constant, irrespective of experimental temperature. Solute permeabilities, however, increased with temperature. The dependency was larger for larger solutes and membranes with smaller pore diameters. Therefore, the hindered diffusion of solutes through micropores was indicative of an activated process. Moreover, pure water permeability, after correction for the temperature effect on viscosity, also increased with experimental temperature.

Introduction

Nanofiltration (NF) membranes, which can be defined as membranes rejecting solutes smaller than about 2 nm (Koros et al., 1994), can be categorized to be between conventional reverse osmosis and ultrafiltration membranes and have molecular weight cutoff (MWCO) in the range of 200 to 1000. NF membranes have considerable potential for application to a variety of separations such as ultrapure water production (Rautenbach and Gröschl, 1990; Petersen, 1993). At present, NF membranes are commercially manufactured from polymeric materials, especially, poly(amide) (Bowen and Mohammad, 1998; Petersen, 1993; Tsuru et al., 1994). Recently, however, inorganic nanofiltration membranes have attracted much attention, since inorganic materials have many advantages over polymeric materials, such as stability at high temperature and resistance to organic solvents. In terms of thermal stability, the maximal operating temperature of commercial NF membranes has been reported to be 40°C, while inorganic materials would be expected to be stable at higher temperatures. Therefore, the utilization of NF membranes at high temperature represents a large advantage for inorganic membranes. The successful preparation of ceramic NF membranes has been recently reported by sol-gel methods using various types of metal oxides, including γ-alumina (Larbot et al., 1994), zirconia (Vacassy et al., 1997), titania (Soria and Cominotti, 1996; Rios et al., 1996), and silica-zirconia composite oxide (Tsuru, 1998a,b). Such membranes have been utilized for the separation of neutral solutes and electrolytes in aqueous solutions.

From the viewpoint of the transport mechanism of NF membranes, most transport models are based on two mechanisms: sieving effect and charge effect. In terms of the charge effect, electrostatic force between the membranes and ions in the feed solutions can play an important role in rejecting electrolytes since NF membranes have pore diameters in a range of a few nanometers (Tsuru et al., 1994). The present work is restricted to a system for the nanofiltration of neutral solutes, that is, the sieving effect. Solutes that permeate through the pores can be transported by diffusive and con-

Correspondence concerning this article should be addressed to T. Tsuru.

vective flow. Both contributions are restricted in comparison with those in the bulk solution, and this is referred to as ''hindered diffusion'' or ''restricted diffusion.''

The theory of hindered diffusion in liquid-filled pores has been investigated using polymeric and inorganic track-etched membranes that have a cylindrical uniform pore structure (Deen, 1987). The track-etched membranes have diameters in a range of 4 to 100 nm, which is a range typical for ultrafiltration and microfiltration membranes. The theory has been extended to NF membranes that have pore diameters as small as 1 nm (Wang et al., 1995; Bowen and Mohammad, 1998). However, a more detailed investigation will be required in order to determine whether the theory can be applied to NF membranes with a pore radius of only several times the size of a water molecule. One of the strategies for examining the transport models is to determine the dependency of membrane performances on permeation temperature. The subsequent analysis of membrane transport parameters, such as pure-water permeability, solute permeability, and reflection coefficient, would provide a great deal of insight into our current understanding of the transport mechanism (Nakao, 1986). Nomura et al. (1987) investigated polymeric and inorganic ultrafiltration membranes in a temperature range between 20 and 60°C. For the case of polymeric membranes (polysulphone), the solute permeability increased with temperature more drastically than the diffusivity in the bulk solution, while that of inorganic membranes (γ-alumina) increased only slightly compared with the diffusivity in the bulk solution. A disadvantage of polymeric membranes is that the pore structures such as pore diameters, thickness, and porosity could be altered because of thermal expansion, and therefore it would be difficult to determine the dependency of permeation properties on temperature. On this point, inorganic membranes are promising materials because of their low thermal expansion and stability. To date, however, very few studies on the effect of temperature on inorganic NF membranes have been carried out, probably because of difficulties in the development of nanofiltration ceramic membranes.

Restricted diffusion in liquid-filled microporous materials also has been extensively investigated using porous adsorbents (Kärger and Ruthven, 1992), which can play an important role in catalysis, chromatography, and so on. Seo and Massoth (1985) determined diffusivities of solutes in an *n*-dodecane solution in alumina powder in the temperature range of 25 to 60°C, and formulated the effect of temperature on the restrictive factor. It should be noted, however, that a limited number of articles have reported the effect of temperature on hindered diffusion in both adsorption and membrane separation, although the effect of temperature appears to be very important from the theoretical point of view as well as in practice.

In this article, inorganic NF membranes were prepared using silica-zirconia composite sol solutions. To discuss the transport mechanism through nanoporous membranes, permeation experiments were carried out at different temperatures. Rejection dependency was analyzed based on the Spiegler-Kedem equation, and the dependency of transport parameters, reflection coefficient, solute permeability, and pure-water permeability, on permeation temperature are discussed.

Theory

Transport equation through membrane

Volume flux (J_v) and solute flux (J_s) through a membrane was formulated by Kedem and Katchalsky (1961) based on irreversible thermodynamics as follows:

$$J_v = L_p(\Delta P - \sigma\Delta\pi) \tag{1}$$

$$J_s = \omega\Delta\pi + (1-\sigma)\bar{C}J_v, \tag{2}$$

where L_p, ω, and σ represent the pure-water permeability, solute permeability, and reflection coefficient, respectively. Spiegler and Kedem (1966) modified Eq. 2 into a differential form of Eq. 3, since the difference in concentrations on both sides of a membrane in reverse osmosis and ultrafiltration may be too large for obtaining $\bar{C}$, which is defined as a logarithmic average of these concentrations:

$$J_s = -D_{\text{eff}}\frac{d}{dx}C + (1-\sigma)CJ_v, \tag{3}$$

where the first and second terms show the contribution of diffusion and convection to solute flux, respectively. Equation 3 represents the ordinal Fickian equation for dilute solutions with modified diffusion and convection terms; D_{eff} is the effective diffusivity inside a membrane and is reported to be different from that in the bulk solution because of hindered diffusion (Nakao, 1986; Deen, 1987); σ is the reflection coefficient, which can be interpreted as the fraction of solute reflected by the membrane in convective flow. By integration of Eq. 3 from feed solution to permeate stream using reverse osmosis conditions ($J_s = C_p J_v$), rejection, which is defined as $R = 1 - C_p/C_f$, can be expressed with the following equations:

$$R = \frac{(1-F)\sigma}{1-\sigma F} \qquad F = \exp\left(-\frac{(1-\sigma)J_v}{P}\right), \tag{4}$$

where solute permeability, P, which is expressed as $P = \omega RT$ for dilute solutions (Nakao, 1986), can be interpreted as $D_{\text{eff}}/\Delta x$, that is, effective diffusivity divided by membrane thickness Δx. It should be noted that the transport equations derived by Deen (1987) are expressed in a similar manner to the Spiegler-Kedem equation.

The membrane parameters have been interpreted based on several transport models. According to the pore model (Nakao, 1986), the transport membrane parameters of a rigid spherical solute (diameter = d_s) permeating through a capillary (diameter = d_p) without specific interaction between them has been formulated based on hydrodynamic analysis (Nakao, 1986; Deen, 1987). The membrane transport parameters can be expressed as follows, using the ratio of solute diameters over membrane pore diameters, q (Nakao, 1986):

$$L_p = \frac{r_p^2}{8\mu}\frac{A_k}{\Delta x} \tag{5}$$

$$\sigma = 1 - S_F\left\{1 + \left(\frac{16}{9}\right)q^2\right\} \tag{6}$$

$$P = D_{\text{bulk}}S_D\frac{A_k}{\Delta x} \tag{7}$$

$$S_F = 2(1-q)^2 - (1-q)^4, \qquad S_D = (1-q)^2, \qquad (8)$$

where A_k is the porosity of a membrane. It should be noted that σ is a function of q, that is, it is defined using structural parameters. On the other hand, P is expressed using the effective diffusivity inside a pore, $D_{\text{eff}} = D_{\text{bulk}} S_D$: the product of a structural parameter S_D and a kinetic property (diffusivity).

Concentration polarization

When one of the feed components is rejected, concentration polarization occurs outside a membrane. Solutes that are rejected by a membrane accumulate on the outer surface of the feed solution, and therefore the concentration at the interface (C_m) becomes larger than the feed concentration. Two types of rejection, that is, an observed rejection R_{obs} ($=1-C_p/C_b$) and a real rejection R_{real} ($=1-C_p/C_m$) can be defined (Nakao, 1986; Mitchell and Deen, 1986). R_{real} should be used for a discussion of membrane permeation properties. The effect of concentration polarization is hydrodynamic, and can be analyzed using mass-transfer coefficient, k, as follows:

$$\frac{C_m - C_p}{C_b - C_p} = \exp\left(\frac{J_v}{k}\right). \qquad (9)$$

Equation 9 can be transformed into R_{obs} and R_{real} as follows:

$$\ln\frac{1-R_{\text{obs}}}{R_{\text{obs}}} = \ln\frac{1-R_{\text{real}}}{R_{\text{real}}} + \frac{J_v}{k}. \qquad (10)$$

For the case of a stirred cell, the dependency of k can be expressed as follows using agitation speed ω:

$$k = a\omega^b, \qquad (11)$$

where a and b are a constant value and are dependent on the geometry of the experimental cells. For the case of a stirred cell, b can be successfully assumed to be 0.567 (Bowen et al., 1997). By measuring R_{obs} at different agitation speed with constant J_v, a linear plot of $\ln\{(1-R_{\text{obs}})/R_{\text{obs}}\}$, as a function of $J_v/\omega^{0.567}$, gives a and R_{real} as the slope and the intersect of the y-axis.

Experimental Studies

Preparation of inorganic nanofiltration membranes

Inorganic NF membranes were prepared using a sol-gel process; a silica-zirconia composite colloidal sol solution was coated on α-alumina porous substrate (outer diameter 1 cm, length 9 cm) and fired at 570°C. The pore size of the porous membranes can be controlled via the choice of an appropriate colloidal diameter of sol solution. The procedure is described in a previous paper (Tsuru et al., 1998b). Several membranes, which had molecular weight cutoffs in a range of approximately 200 to 1000 were used for the present study. Three membranes, denoted as M-1, -2, and -3, were used for an investigation of the effect of applied pressure and temperature on nanofiltration performance, while the remainders, denoted as M-A and -B, were for investigation of concentration polarization effects.

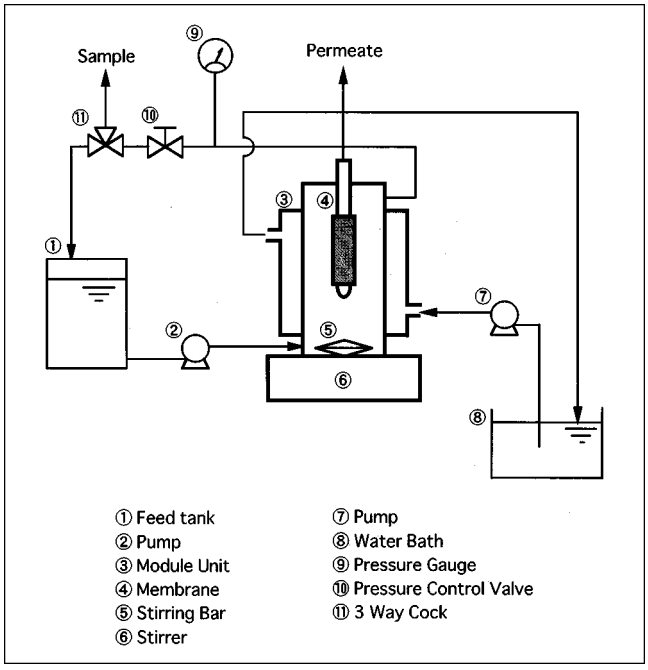

Figure 1. Experimental apparatus for nanofiltration experiment.

Nanofiltration experiment

Figure 1 shows an NF experimental apparatus. A porous inorganic membrane with both ends connected with glass tubing was installed vertically inside a continuous stirred cell with an inner diameter of 4 cm. The permeate was collected using a peristaltic pump. The feed solution, pressurized using a plunger pump in a range from 0.2 to 2 MPa, was agitated using a magnetic stirrer at a speed from 200 to 1,200 rpm and was recycled to the feed tank at an approximate flow rate of 20 cm^3/min. The temperature of the feed solution was kept at 20°C to 50°C using a water bath; the highest temperature was limited to 50°C because the membrane cell was made of acrylic resin. The solutes used were various types of neutral organic compounds: alcohols [methanol (MW 32), ethanol (46), *n*-butanol (74)], sugars [*D*-glucose (180), *D*-maltose (342), raffinose (504), α-cyclodextrin (973), and γ-cyclodextrin (1297)], and polyethylene glycols [PEG 3000 (3400) and PEG 6000 (6800)]. These solutes are abbreviated hereafter as MeOH, EtOH, BuOH, Glu, Mal, α-CD, and γ-CD. The feed concentrations were maintained at approximately 500 ppm to prevent flux change due to osmotic pressure. The concentrations in feed and permeate (C_b, C_p) were determined by liquid chromatography and a refractive index detector, which were used for calculating observed rejection, R_{obs}.

The experimental procedures for investigating the effect of applied pressure and temperature on rejection and permeate volume flux were as follows. First, rejection and permeate volume flux for a solution of a certain solute were measured by changing the applied pressure at 25°C, and then measured at higher temperatures up to 50°C. The same procedures were carried out for the different solutes.

Result and Discussion

Concentration polarization

Figure 2 shows volume flux, J_v, and observed rejection, R_{obs}, as a function of stirring speed ω at a constant applied pressure of 1.0 MPa. Observed rejection R_{obs} increased with increasing stirring speed because a higher stirring speed can reduce the polarization effect and consequently increase R_{obs}. On the other hand, the permeate volume flux was nearly constant irrespective of ω and types of solutes because of the low feed concentrations. In Figure 3 $\ln\{(1-R_{obs})/R_{obs}\}$ is plotted as a function of $J_v/\omega^{0.567}$ according to Eq. 10. The relation could be expressed as a linear plot, and the dependency of the mass-transfer coefficient on stirring speed, that is, $a=0.567$, is appropriate. Real rejection R_{real} can be obtained by extrapolation to the ordinate axis. On the other hand, the mass-transfer coefficient, k, can be obtained by the slope of the plot, and summarized as Sh using Schmidt (Sc) and Reynolds (Re) numbers as shown in Figure 4. Various solutes were well correlated as

$$Sh = \frac{kd}{D} = 0.25 Re^{0.567} Sc^{0.33}. \qquad (12)$$

By using Eqs. 10 and 12, R_{obs}, which is experimentally obtained, can be converted together with J_v into R_{real}, which represents a real rejection based on the concentration at the feed surface. Equation 12 was applied at different temperatures by considering the change in viscosity and diffusivity. Diffusivity of solutes at low concentration can be predicted with the following Wilke-Chang equation (Reid et al., 1977):

$$D = \text{const}\frac{T}{\mu}. \qquad (13)$$

A constant term in Eq. 13 involves the properties of the solutes that are predictable and independent of temperature. Table 1 summarizes the diffusivities of solutes calculated from Eq. 13 and the Stokes radii.

Figure 5 shows the volume permeate flux, J_v, and rejections (both R_{obs} and R_{real}) as a function of applied pressure. Permeate volume flux increases linearly with applied pres-

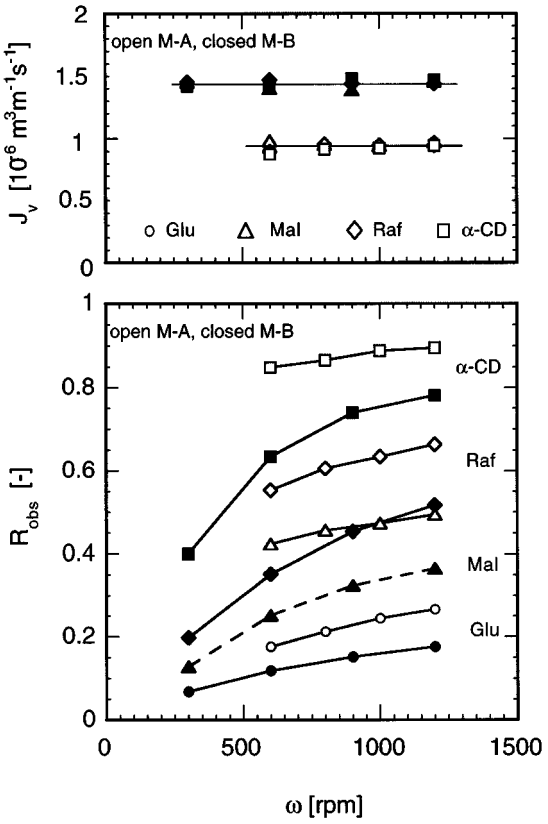

Figure 2. Volume flux (J_v) and observed rejection (R_{obs}) as a function of agitation speed (ω) at an applied pressure of 1.0 MPa.

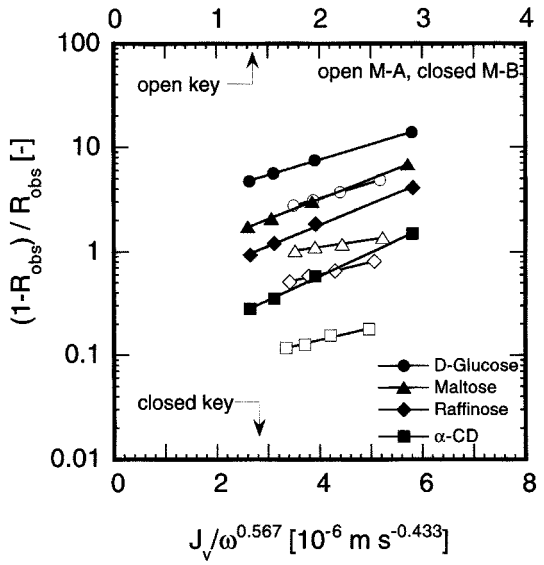

Figure 3. Plot of $\ln\{(1-R_{obs})/R_{obs}\}$ as a function of $J_v/\omega^{0.567}$.

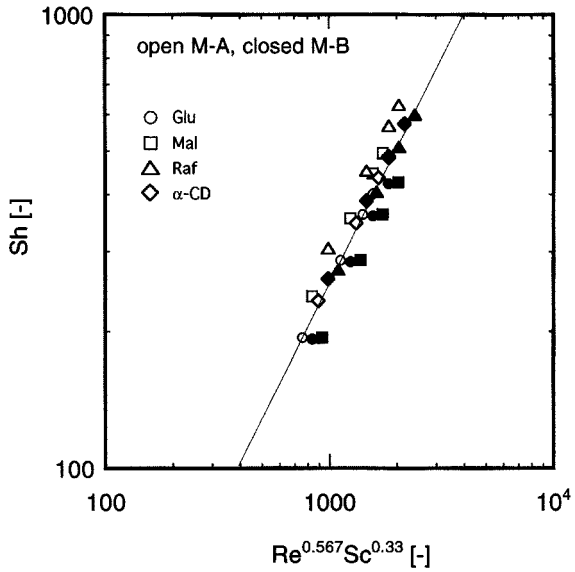

Figure 4. *Sh* as a function of $Re^{0.567}Sc^{0.33}$.

Table 1. Diffusivities and Stokes Radii of Solutes

	MW	r_s	Diffusivity [10^{-9} m$^2\cdot$s^{-1}]				
	[g·mol^{-1}]	[nm]	20°C	25°C	30°C	40°C	50°C
Methanol	32	0.137		1.79		2.56	3.15
Ethanol	46	0.167		1.47		2.10	2.59
n-Butanol	74	0.234		1.05		1.50	1.85
1-Hexanol	102	0.568		0.846		1.21	1.49
Glucose	180	0.307		0.8		1.15	1.41
Maltose	342	0.452	0.474	0.542	0.616	0.777	0.957
Raffinose	504	0.568	0.377	0.432	0.490	0.618	0.761
α-Cyclodextrin	972	0.840	0.252	0.29	0.328	0.414	0.510
γ-Cyclodextrin	1297	1.00	0.212	0.242	0.276	0.348	0.429

sure, while rejection increases with applied pressure and appears to reach a constant rejection, as is often reported in the literature (Nakao, 1986). According to Eq. 3, solute flux, which can be expressed as $J_s = (1-R)C_m J_v$, is dominated by diffusion for low permeate volume flux. On the other hand, solute flux at large J_v is transported mainly by convection, and therefore rejection approaches σ for a large volume flux (Deen, 1987).

Temperature dependency of nanofiltration performances

The evaluation of NF performances, that is, measurement of permeate volume flux and rejection, which reflect the membrane characteristics, was carried out using neutral solutes of a variety of molecular weights. Figure 6 shows J_v and R_{obs} as a function of molecular weights of solutes that were

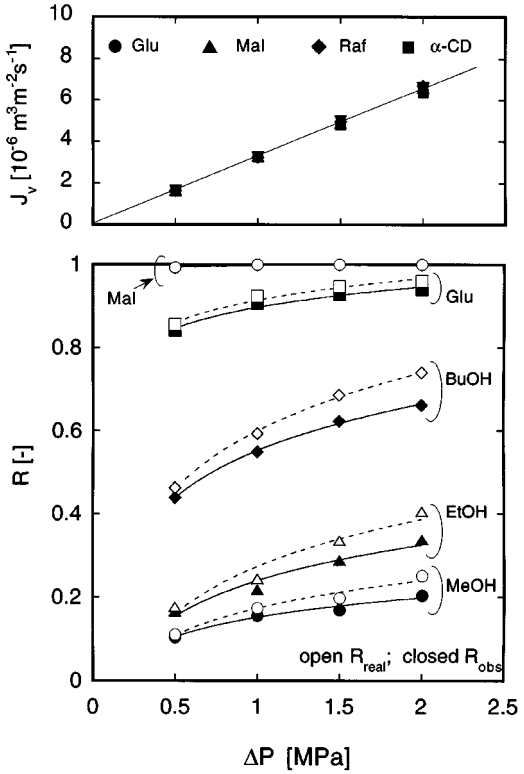

Figure 5. Volume flux, J_v, observed (R_{obs}), and real rejection (R_{real}) as a function of applied pressure (M1, 25°C).

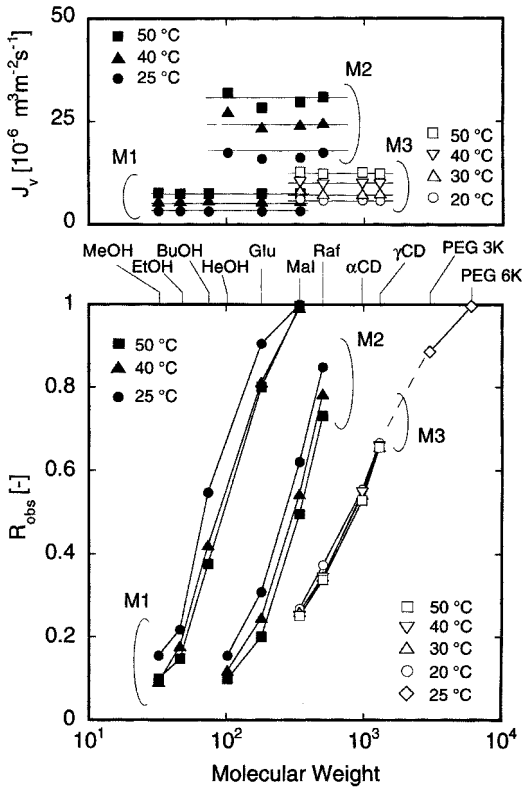

Figure 6. Volume flux and observed rejection as a function of molecular weights of solutes (M1, M2, and M3, silica-zirconia membranes, $\Delta P = 1$ MPa).

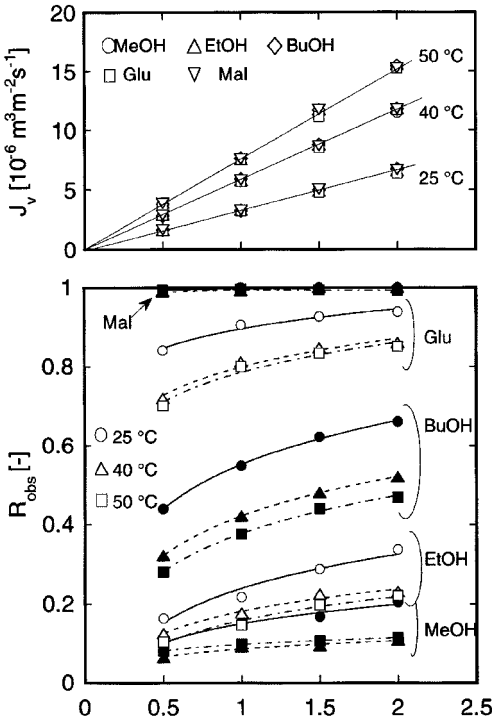

Figure 7. Volume flux and rejection as a function of applied pressure (M1; 25, 40 and 50°C).

measured at 1.0 MPa for membranes M1, M2, and M3. The rejection curves are so-called MWCO curves, which reflect the effective pore size, were controlled by colloidal diameters at the final coating (Tsuru et al., 1998a), are sufficiently sharp for selective separation. MWCOs defined at 90% rejection are approximately 200, 600, and 2,000, respectively. Observed rejection, R_{obs}, decreases with permeation temperature. It should be noted that the rejection of maltose by M1 was nearly 100% irrespective of permeation temperature, and therefore the pore diameter appears to be unchanged in this experimental range. This is in contrast to the case of polymeric membranes whose pore diameters are often enlarged at high temperatures. On the other hand, the volume flux of permeate was not dependent on the types of solutes because of low feed concentration, as can be seen by Eq. 1, but was dependent on permeation temperature.

Figure 7 shows permeate volume flux and observed rejection for M1 at 25, 40 and 50°C as a function of applied pressure. The permeate volume flux increases with applied pressure as well as permeation temperature, while the dependency on the types of solutes seems to be negligible. In this experiment, a feed solution of 50°C was supplied at the maximal pressure of 2 MPa at least 5 times, according to the experimental procedure. Therefore, the present NF membranes were found to be quite stable in this temperature range and applied pressure. It should be noted that most NF membranes prepared from polymeric materials must be used below 40°C (Petersen, 1993). In terms of rejection, R_{obs} decreases with an increase in permeation temperature, irrespective of types of solutes. On the other hand, R_{obs} increases with applied pressure, irrespective of the permeation temperature.

To discuss the solute permeation through NF membranes, R_{real} was obtained after correction of concentration polarization by using Eqs. 10 and 12, and therefore we are able to discuss the solute permeation mechanism through a membrane by excluding the effect of concentration polarization. Real rejection, R_{real}, is plotted as a function of $1/J_v$ for M1, M2, and M3, in Figures 8a, 8b, and 8c, respectively. Curves in the figure are calculated with Eq. 4 using fitted membrane

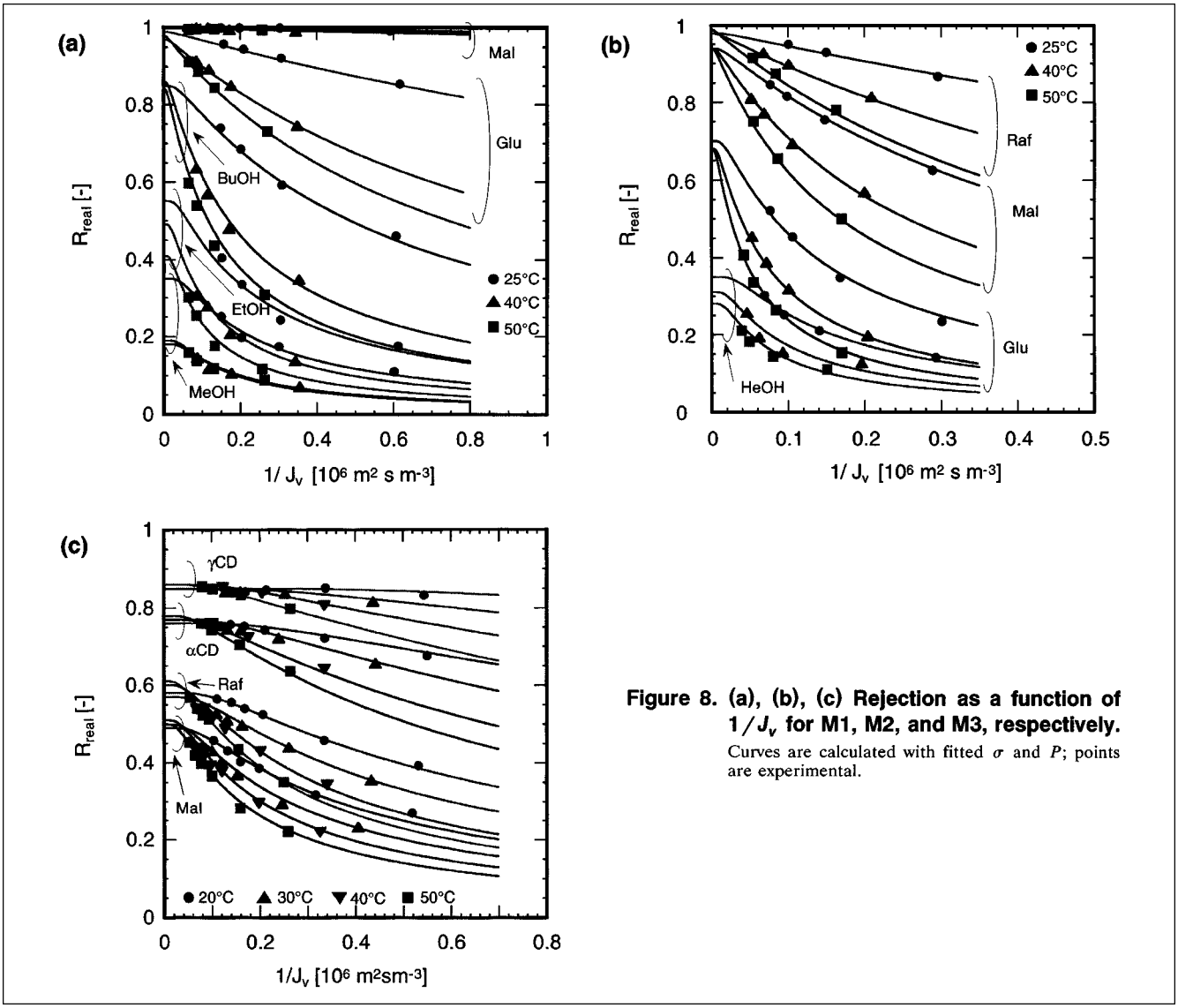

Figure 8. (a), (b), (c) Rejection as a function of $1/J_v$ for M1, M2, and M3, respectively.

Curves are calculated with fitted σ and P; points are experimental.

Table 2. Fitted σ and P [10^{-6} m·s^{-1}] for M1, M2, and M3

(*a*)		25°C		40°C		50°C	
	M1	σ	P	σ	P	σ	P
	Methanol	0.35	4.58	0.19	6.67	0.18	5.8
	Ethanol	0.55	4.23	0.49	8.46	0.41	10.2
	Butanol	0.85	1.58	0.86	4.6	0.84	6.5
	Glucose	0.99	0.27	0.97	0.90	0.98	1.3
	Maltose	1	0.01	1	0.017	1	0.02
(*b*)		25°C		40°C		50°C	
	M2	σ	P	σ	P	σ	P
	Hexanol	0.35	6.58	0.31	11.15	0.28	13.8
	Glucose	0.70	6.5	0.68	13.0	0.68	20
	Maltose	0.94	1.8	0.94	3.54	0.94	5.40
	Raffinose	0.98	0.45	0.98	1.06	0.99	1.77

(*c*)	20°C		30°C		40°C		50°C	
M3	σ	P	σ	P	σ	P	σ	P
D-Maltose	0.49	2.4	0.50	3.46	0.51	4.57	0.50	5.63
Raffinose	0.58	1.30	0.57	1.84	0.60	2.85	0.61	3.70
α-Cyclodextrin	0.76	0.38	0.77	0.60	0.77	0.95	0.78	1.28
γ-Cyclodextrin	0.85	0.10	0.85	0.20	0.86	0.35	0.86	0.52

parameters σ and P, which are summarized in Table 2. It should be noted that the analysis based on the Spiegler-Kedem equation assumes that membranes have homogeneous transport properties, while the pore-size distribution might exist in the present membranes. Figure 9 shows σ and P for M1, M2, and M3 as a function of the molecular weights of the solutes. The σ increases with an increase in the molecular weight of the solutes (the molecular size of solutes) and shows different curves for each membrane. On the other hand, solute permeability decreases with the molecular weight of solutes. It should be noted that the slope of the decrease in permeabilities is larger than that in the bulk diffusivity because of steric effects. The σ can be interpreted as rejection at infinitely high flux, that is, graphically the intercepts at the ordinate of the fitted curves in Figures 8a, 8b, and 8c. It is clear that the dependency of σ on temperature is not as large as that of permeability, except in the case of alcohols. It should be noted that $(1-R)$ can be interpreted as a normalized solute flux using volume flux, J_v, and feed concentration, C_b. Therefore, rejection dependency on temperature can be interpreted as follows. The solute flux was increased more rapidly than volume flux with increasing permeation temperature. Since solute flux can be expressed using two transport parameters σ and P, and since σ is nearly constant irrespective of permeation temperature, the reason for a decreased rejection with temperature is shown to be due to an increase in solute permeabilities. The same conclusion was drawn using inorganic and heat-resistant polymeric ultrafiltration membranes (Nomura et al., 1987). According to the steric-hindrance pore model, σ is simply constant, provided d_s and d_p are constant in Eq. 6. It is, therefore, quite natural that σ shows constant values since inorganic membranes showed excellent stability in the present experimental conditions. On the other hand, a different dependency of σ of the alcohols on temperature from those of sugars might be caused by selective adsorption on the pore wall, which is suggested by larger rejections of alcohols than those of sugars and glycols (Tsuru et al., 1998b).

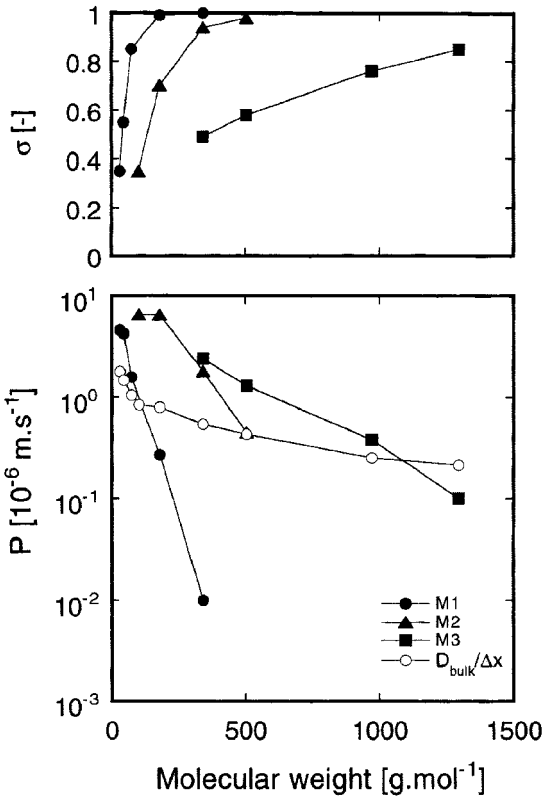

Figure 9. Reflection coefficient (σ) and solute permeability (P) as a function of solute molecular weights.

M1, M2, 25°C; M3, 20°C; $D_{bulk}/\Delta X$ is shown with $\Delta x = 1$ mm for a reference for temperature dependency.

As explained in the theoretical section, the solute permeability P can be interpreted using an effective diffusivity inside a membrane. In order to discuss the temperature dependency of permeability on permeation temperature, the solute permeability P divided by bulk diffusivity, P/D, is plotted in Figure 10 after normalization with that of 20 or 25°C as a function of permeation temperature. If the effective diffusivity inside a pore increases in the same manner as the bulk diffusivity, P/D should be constant. However, P/D increases with an increase in permeation temperature for the three membranes, as shown in the figure. The slopes appear to be dependent on both membrane pore size and solute size. Figure 11 shows an Arrhenius plot of P/D, which gives a relatively linear relationship between P/D with reciprocal temperature in the present experimental range, and therefore the observed activation energies of (P/D), ΔE_p, can be obtained.

Figure 12 summarizes ΔE_p as a function of the reflection coefficient, σ. According to Eq. 6, σ can be converted into the ratio of solute diameter to membrane pore diameter, q, which is shown in Figure 13. Observed activation energy, ΔE_p, with different types of solutes and membranes shows a relatively good correlation with σ and q. ΔE_p appears to be zero for conditions at which $\sigma = 0$ and $q = 0$; in this case, the solutes are very small, and the dependency of the diffusivity through a pore on permeation temperature is the same as

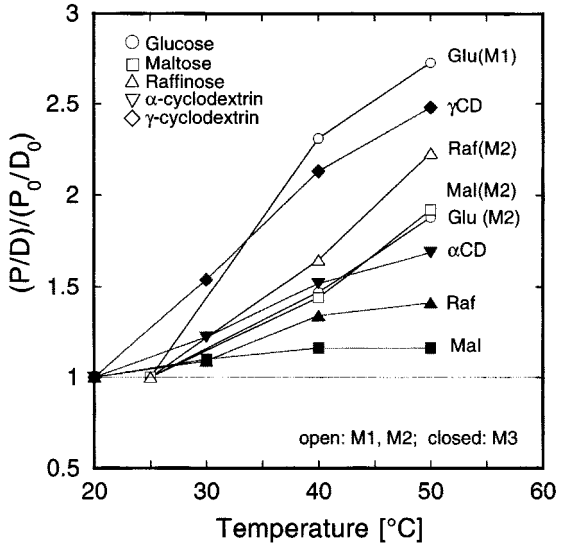

Figure 10. Normalized *P/D* for various molecular-weight sugars as a function of temperature.

P/D is normalized with *P/D* at 20°C for M3 and at 25°C for M1 and M2, respectively.

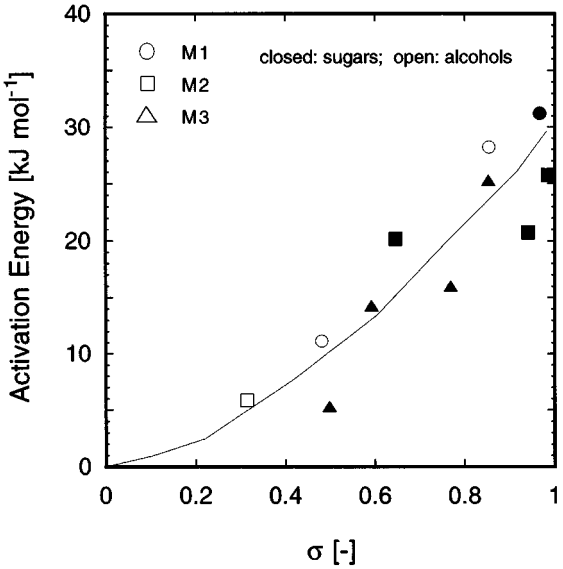

Figure 12. Observed activation energy of normalized permeability as a function of reflection coefficients, σ.

that of bulk solutions. With an increase in σ and q, the observed activation energy, ΔE_p, increases. It should be noted that permeability is expressed as the diffusivity in bulk solution and the structural parameter S_D in Eqs. 7 and 8. However, we see in Figures 12 and 13 that hindered diffusion in a small capillary in a range of NF membranes is an activated process. A small number of articles have addressed the issue of the temperature dependency of hindered diffusivity. The similar dependency of $D_{\text{eff}}/D_{\text{bulk}}$ on temperature has been reported for the diffusion of solutes in *n*-dodecane solutions through alumina adsorbents by Seo and Massoth (1985). Diffusing molecules through pores meets an energy barrier at the entrance of the pores and inside the pore based on hydrodynamic drag forces, and the restrictive diffusion therefore can be considered to be an activated process. The activation energy increases approximately up to 30 kJ·mol^{-1} with σ and q. It should be noted that in the research area of restricted diffusions in adsorption the activation energy of configurational diffusion has been reported to be in the range of 10 ~ 60 kJ·mol^{-1} (Xiao and Wei, 1992).

Figure 14 shows $L_p\mu$ (the permeability of water multiplied by solution viscosity) normalized with that of 20 or 25°C as a function of permeation temperature. In the figure, $L_p\mu$ from inorganic reverse-osmosis membranes, whose pore diameters are estimated to be smaller than NF membranes, is also indi-

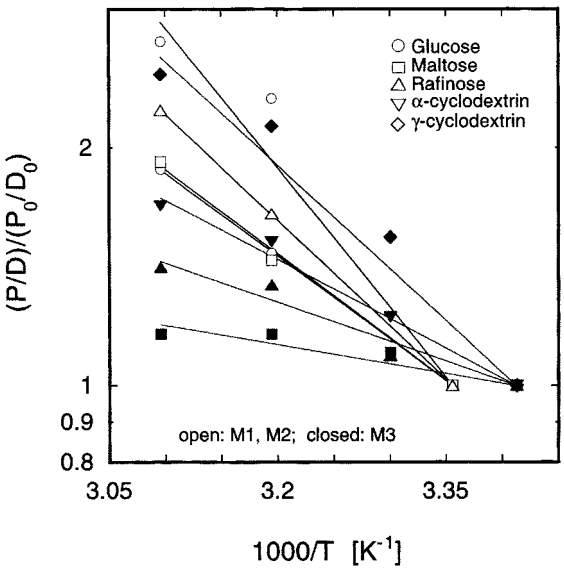

Figure 11. Arrehnius plots of *P/D*.

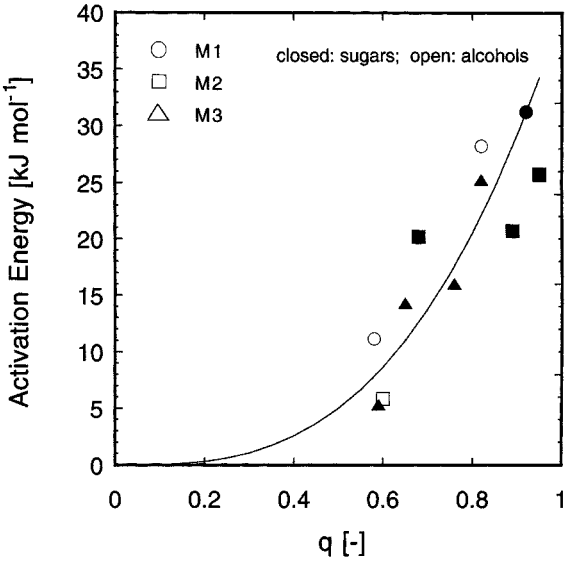

Figure 13. Observed activation energy of normalized permeability as a function of the ratio of molecular diameter of solute to pore diameter of membrane, *q*.

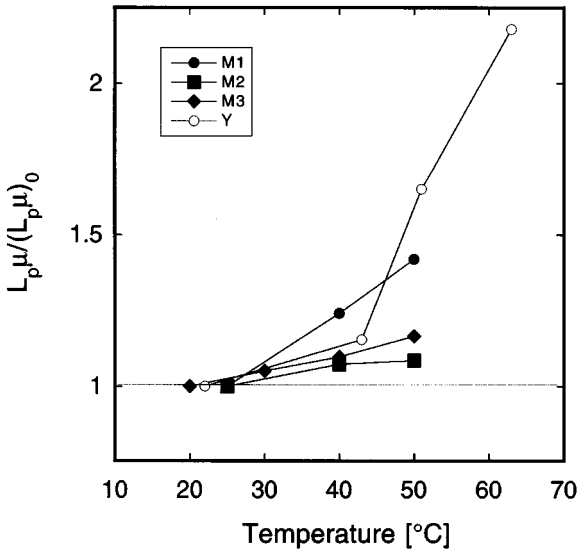

Figure 14. Normalized pure-water permeability as a function of temperature.

$L_p\mu$ is normalized with that at 20°C for M3 and at 25°C for M1 and M2, respectively; data relative to membrane *Y* was taken from Yazawa et al. (1991).

cated (Yazawa et al., 1991). If the water permeation obeys the viscous flow mechanism, $L_p\mu$ should be constant. It is obvious that $L_p\mu$ increases with temperature, and the dependency appears to be larger for membranes having smaller pore diameter. Table 3 summarizes the observed activation energies of pure-water permeability. The transport mechanism of water through membranes with pore diameters smaller than several nm seems to deviate from the viscous flow mechanism. The same tendency has been observed for a system where a nonaqueous solution such as ethanol permeated through silica-zirconia NF membranes (Tsuru et al., 1998c). The reason for this can be explained in several ways. The permeation of water through micropores is an activated process, and hence different from viscous flow; that is, a water molecule is subject to friction from the pore walls in the range of approximately 1 nm. It should be noted that the water molecule is one of the smallest molecules, whose kinetic diameters is reported as 0.29 nm, and in the same range as those of helium (0.24 nm) and hydrogen (0.27 nm) (Breck, 1974). A portion of the water molecules that have sufficient thermal energy to jump the energy barrier from the pore walls can permeate through the pores. Another explanation could be based on the adsorption of water on hydrophilic pore walls. The effective pore diameter for water permeation might be reduced by the adsorbed water. The adsorbed layer can be thinner at higher temperatures, and therefore the effective pore diameter might be larger. Finally, viscosity in fine pores is reported to be different from that of a bulk solution (Drost-Hansen, 1982). Therefore, the dependency of viscosity in micropores might be larger than that of the bulk solution.

Table 3. Observed Activation Energy of Pure Water Permeability*

Membrane	MWCO	ΔE_{pw} [kJ·mol^{-1}]
M1	200	24.6
M2	600	19.0
M3	2,000	18
Y	—	30.5

*L_w in the form of $J_w = L_w \Delta P$.

Ternan (1987) assumed that the viscosity in a small pore could be divided into two parts—bulk viscosity and an incremental contribution caused by proximity of the pore wall—and successfully explained the temperature dependency of diffusivity through adsorbents by relating the diffusivity of solutes and solution viscosity with Eq. 13. However, the viscosity inside a pore was not measured and assumed to be a fitting parameter. It should be noted that the evaluation of permeate flux and rejection in nanofiltration corresponds to the simultaneous measurement of the diffusivity of solutes and the viscosity of solution through pores. In the present case, if J_v increased with temperature in the same manner as *P*, rejection should be constant according to Eq. 4. Therefore, a decrease in rejection indicates that the dependence of diffusivity on temperature cannot be interpreted solely by a change in viscosity of the pores. Permeation mechanism involves structural properties (such as pore size, pore shape, pore length, solute size, solute shape) as well as physicochemical properties (such as hydrophilicity/hydrophobicity, zeta potential). The present results might be drawn for the system of silica-zirconia membranes prepared by the sol-gel procedure. Therefore, at present, we cannot deduce the reason why solute diffusivity and water permeability are dependent on temperature. It is clear, however, that the dependence was caused by interaction between permeating molecules and pore surfaces with a pore diameter of less than a few nm.

Conclusions

Inorganic porous membranes with MWCO of approximately 200, 600, and 2,000 were used in nanofiltration experiments of neutral solutes at different temperatures. The rejection dependency on volume flux was analyzed based on the Spiegler-Kedem equation, which considers the contribution of convection and diffusion to solute flux. The reflection coefficient that corresponds to the fraction of solutes reflected by the membrane in convective flow was nearly constant irrespective of experimental temperature. However, permeabilities increased with temperature. The dependence of permeabilities on temperature was greater for larger solutes and for the case of membranes with a smaller pore diameter. The activation energy increased with larger values of *q*, ratios of solute diameter to membrane pore diameter, up to 30 kJ·mol^{-1}. It has been suggested that the hindered diffusion of solutes through micropores is an activated process. Moreover, pure-water permeability, after correlation for the effect of temperature on viscosity, also increased with temperature in the experiment. An activated process is indicated for the permeation of water, which consists of one of the smallest molecules.

Notation

C = concentration, mol·m^{-3}
D_{bulk} = bulk diffusivity, m^2·s^{-1}
d = diameter of stirring bar, m
J_w = water flux, mol·m^{-2}·s^{-1}

L_w = pure water permeability, $mol \cdot m^{-2} \cdot s^{-1} \cdot Pa^{-1}$
q = ratio of solute diameter to capillary diameter ($= d_s/d_p$)
$\Delta\pi$ = osmotic pressure, Pa
μ = viscosity, $Pa \cdot s$
ρ = density of solution, $kg \cdot m^3$

Subscripts

b = bulk
f = feed
m = membrane surface
p = permeate

Literature Cited

Bowen, W. R., and A. W. Mohammad, ''Characterization and Prediction of Nanofiltration Membrane Performance—A General Assessment,'' *Trans. Inst. Chem. Eng*., **76**, 885 (1998).

Bowen, W. R., A. W. Mohammad, and N. Hilal, ''Characterization of Nanofiltration Membranes for Predictive Purpose—Use of Salts, Uncharged Solutes and Atomic Force Microscopy,'' *J. Memb. Sci*., **126**, 91 (1997).

Breck, D. W., *Zeolite Molecular Sieves*, Wiley, New York, p. 636 (1976).

Deen, W. M., ''Hindered Transport of Large Molecules in Liquid-Filled Pores,'' *AIChE J*., **33**, 1409 (1987).

Drost-Hansen, W., ''The Occurrence and Extent of Vicinal Water,'' *Biophysics of Water*, F. Franks and S. Mathias, eds., Wiley, New York, p. 163 (1982).

Kärger, J., and D. M. Ruthven, *Diffusion in Zeolites and Other Microporous Solids*, Wiley, New York (1992).

Kedem, O., and A. Katchalsky, ''A Physical Interpretation of the Phenomenological Coefficients of Membrane Permeability,'' *J. Gen. Physiol*., **45**, 143 (1961).

Koros, W. J., Y. H. Ma, and T. Shimizu, ''Terminology for Membranes and Membrane Process (IUPAC Recommendations 1996),'' *J. Memb. Sci*., **120**, 149 (1994).

Larbot, A., S. Alami-Younssi, M. Persin, J. Sarrazin, and L. Cot, ''Preparation of γ-Alumina Nanofiltration Membrane,'' *J. Memb. Sci*., **97**, 167 (1994).

Mitchell, B. D., and W. M. Deen, ''Effect of Concentration on the Rejection Coefficients of Rigid Macromolecules in Track-Etch Membranes,'' *J. Colloid Interface Sci*., **113**, 1132 (1986).

Nakao, S., ''Membrane Transport Phenomena and Ultrafiltration,'' *Encyclopedia of Fluid Mechanics*, Gulf Pub., Houston, p. 987 (1986).

Nomura, T., S. Nakao, and S. Kimura, ''Influence of Feed Temperature on Ultrafiltration Performance,'' *Kagaku Kogaku Ronbunshu*, **13**, 811 (1987).

Petersen, R., ''Composite Reverse Osmosis and Nanofiltration Membranes,'' *J. Memb. Sci*., **83**, 81 (1993).

Rautenbach, R., and A. Gröschl, ''Separation Potential of Nanofiltration Membranes,'' *Desalination*, **77**, 73 (1990).

Reid, R., J. Prausnitz, and T. Sherwood, *The Properties of Gasses and Liquids*, 3rd ed., McGraw-Hill, New York (1977).

Rios, G. M., R. Joulie, S. J. Sarrade, and M. Carlès, ''Investigation of Ion Separation by Microporous Nanofiltration Membranes,'' *AIChE J*., **42**, 2521 (1996).

Seo, G., and F. E. Massoth, ''Effect of Pressure and Temperature on Restrictive Diffusion of Solutes in Aluminas,'' *AIChE J*., **31**, 494 (1985).

Soria, R., and S. Cominotti, ''Nanofiltration Ceramic Membrane,'' *Proc. ICOM96*, Yokohama, Japan, 469 (1996).

Spiegler, K. S., and O. Kedem, ''Thermodynamics of Hyperfiltration (Reverse Osmosis) Criteria for Efficient Membranes,'' *Desalination*, **1**, 311 (1966).

Ternan, M., ''The Diffusion of Liquid in Pores,'' *Can. J. Chem. Eng*., **60**, 244 (1987).

Tsuru, T., T. Shutou, S. Nakao, and S. Kimura, ''Peptide and Amino Acid Separation by Nanofiltration Membranes,'' *Sep. Sci. Technol*., **29**, 971 (1994).

Tsuru, T., H. Takezoe, and M. Asaeda, ''Ion Separation by Porous Silica-Zirconia Nanofiltration Membrane,'' *AIChE J*., **4**, 765 (1998a).

Tsuru, T., S. Wada, S. Izumi, and M. Asaeda, ''Silica-Zirconia Membranes for Nanofiltration,'' *J. Memb. Sci*., **149**, 127 (1998b).

Tsuru, T., T. Sudoh, S. Kawahara, T. Yoshioka, and M. Asaeda, ''Inorganic Microporous Membranes for Nanofiltration in Non-Aqueous Solutions,'' *Proc. Int. Conf. on Inorg. Memb*., Nagoya, Japan, p. 314 (1998c).

Vacassy, R., C. Guizard, V. Thoraval, and L. Cot, ''Synthesis and Characterization of Microporous Zirconia Powers: Application in Nanofiltration and Nanofiltration Characteristics,'' *J. Memb. Sci*., **132**, 109 (1997).

Wang, X. L., T. Tsuru, S. Nakao, and S. Kimura, ''The Electrostatic and Steric-Hindrance Model for the Transport of Charged Solutes Through Nanofiltration Membranes,'' *J. Memb. Sci*., **135**, 19 (1997).

Xiao, J., and J. Wei, ''Diffusion Mechanism of Hydrocarbons in Zeolites—1. Theory,'' *Chem. Eng. Sci*., **47**, 1123 (1992).

Yazawa, T., T. Tanaka, H. Nakamichi, and T. Yokoyama, ''Preparation of Water and Alkali Durable Porous Glass Membrane Coated on Porous Alumina Tubing by Sol-Gel Methods,'' *J. Memb. Sci*., **60**, 307 (1991).

Manuscript received May 14, 1999, and revision received Oct. 25, 1999.